Atmos. Chem. Phys. Discuss., 9, 25049–25084, 2009
www.atmos-chem-phys-discuss.net/9/25049/2009/

Atmospheric Chemistry and Physics Discussions

This discussion paper is/has been under review for the journal Atmospheric Chemistry and Physics (ACP). Please refer to the corresponding final paper in ACP if available.

Tracer measurements in the tropical tropopause layer during the AMMA/SCOUT-O3 aircraft campaign

C. D. Homan[1,*], C. M. Volk[1,*], A. C. Kuhn[1], A. Werner[1], J. Baehr[1], S. Viciani[2], A. Ulanovski[3], and F. Ravegnani[4]

[1]Institute for Atmospheric and Environmental Sciences, Goethe University Frankfurt, Germany
[2]Istituto Nazionale di Ottica Applicata, Florence, Italy
[3]Central Aerological Observatory, Dolgoprudny, Russia
[4]CNR Institute of Atmospheric Science and Climate, Bologna, Italy
[*]now at: Department of Physics, University of Wuppertal, Germany

Received: 29 September 2009 – Accepted: 12 November 2009 – Published: 25 November 2009

Correspondence to: C. D. Homan (c.homan@iau.uni-frankfurt.de)

Published by Copernicus Publications on behalf of the European Geosciences Union.

Abstract

We present airborne in situ measurements made during the AMMA (African Monsoon Multidisciplinary Analysis)/SCOUT-O3 campaign between 31 July and 17 August 2006 on board the M55 Geophysica aircraft, based in Ouagadougou, Burkina Faso. CO_2 and N_2O were measured with the High Altitude Gas Analyzer (HAGAR), CO was measured with the Cryogenically Operated Laser Diode (COLD) instrument, and O_3 with the Fast Ozone ANalyzer (FOZAN). We analyze the data obtained during five local flights to study the dominant transport processes controlling the tropical tropopause layer (TTL) above West-Africa: deep convection up to the level of main convective outflow, overshooting of deep convection, horizontal inmixing across the subtropical tropopause, and horizontal transport across the subtropical barrier. Except for the flight of 13 August, distinct minima in CO_2 indicate convective outflow of boundary layer air in the TTL. The CO_2 profiles show that the level of main convective outflow was mostly located between 350 and 360 K, and for 11 August reached up to 370 K. While the CO_2 minima indicate quite significant convective influence, the O_3 profiles suggest that the observed convective signatures were mostly not fresh, but of older origin. When compared with the mean O_3 profile measured during a previous campaign over Darwin in November 2005, the O_3 minimum at the main convective outflow level was less pronounced over Ouagadougou. Furthermore O_3 mixing ratios were much higher throughout the whole TTL and, unlike over Darwin, rarely showed low values observed in the regional boundary layer. Signatures of irreversible mixing following overshooting of convective air were scarce in the tracer data. Some small signatures indicative of this process were found in CO_2 profiles between 390 and 410 K during the flights of 4 and 8 August, and in CO data at 410 K on 7 August. However, the absence of expected corresponding signatures in other tracer data makes this evidence inconclusive, and overall there is little indication from the observations that overshooting convection has a profound impact on TTL composition during AMMA. We find the amount of photochemically aged air isentropically mixed into the TTL across the subtropical tropopause to

ACPD

9, 25049–25084, 2009

be not significant. Using the N_2O observations we estimate the fraction of aged extratropical stratospheric air in the TTL to be 0.0±0.1 up to 370 K during the local flights, increasing above this level to 0.2±0.15 at 390 K. The subtropical barrier, as indicated by the slope of the correlation between N_2O and O_3 between 415 and 490 K, does not appear as a sharp border between the tropics and extratropics, but rather as a gradual transition region between 10 and 25° N latitude where isentropic mixing between these two regions may occur.

1 Introduction

The tropical tropopause layer (TTL), the region in the tropics where air has characteristics of both the stratosphere and the troposphere, is a critical region of the atmosphere. It is the main region for air entering the stratosphere and therefore it sets the chemical boundary conditions for the stratosphere. The TTL is commonly defined as the layer extending from the level of main convective outflow at 10–14 km to the cold point tropopause at about 16–19 km altitude (Gettelman and Forster, 2002). Laterally, the TTL is bounded by the position of the subtropical jets. Processes active in the TTL include the global-scale circulations in the stratosphere (Brewer-Dobson) and troposphere (Hadley-Walker), large-scale and small-scale atmospheric waves, convection organized on all time and space scales, mixing, radiative heating and cooling, chemistry and cloud microphysics. Satellite observations and 2-D or 3-D transport models provide a general picture of the TTL, but typically cannot well resolve spatial, in particular vertical, variations within the layer. Hence, highly resolved in situ measurements of trace gases and their use as tracers of atmospheric transport have proven extremely useful for studying the radiative, chemical, and dynamical properties of the TTL (e.g., Park et al., 2007). Tracers are compounds whose lifetimes are longer than the timescales of the processes transporting them, such that their distributions are mainly determined by dynamical processes. In the stratosphere, the correlation between two long-lived tracers (tracer-to-tracer correlation) often turns out to be very compact (Plumb and Ko, 1992). The form and curvature of the correlation curve is

ACPD
9, 25049–25084, 2009

dependent on the lifetimes of the tracers and on transport processes. Different atmospheric regions may exhibit different correlation curves between tracers. Variations from these correlations may be caused by horizontal or vertical mixing between the regions or by chemistry. Hence, tracer-to-tracer correlations are a particularly useful tool to study transport and mixing between the troposphere and the stratosphere (e.g., Hoor et al., 2002), or between the tropical and extratropical stratosphere (e.g., Volk et al., 1996). Over the last two decades various field campaigns have taken place to obtain in situ observations of the TTL and get more insight into the different processes taking place in this layer of the atmosphere. Marcy et al. (2007) have presented measurements of HCL, O_3, HNO_3, H_2O, CO, CO_2 and CH_3Cl in the tropical upper troposphere and lower stratosphere (UT/LS) during the Pre-AVE campaign over Costa Rica in January 2004. They infer that a significant amount of stratospheric air and O_3 were present in the TTL, making it distinct from both the stratosphere and the remainder of the troposphere. Park et al. (2007) have presented CO_2 measurements during the Pre-AVE, CR-AVE and TWP-ICE campaign in Costa Rica and Australia. They suggest that the TTL is composed of two layers, the lower TTL which is subject to significant inputs of convective outflow, and the upper TTL, where air ascends slowly and ages uniformly. They calculate a mean age of air entering the lower stratosphere of 26 days during NH winter. Tuck et al. (2003) have analyzed tracers and thermodynamical data from various ER-2 and WB57F aircraft campaigns and documented significant transport from the lower midlatitudes stratosphere toward the tropics, coming to the conclusion that the characteristics of the TTL are determined by a trade-off between subtropical jet stream dynamics and inner tropical ascent via deep convection. Until now, in situ measurements of tracers throughout the TTL have not been reported during NH summer and none have been made above the African continent. However, this region may play an important role in troposphere-to-stratosphere transport. Ricaud et al. (2007) present satellite data of N_2O, CH_4 and CO and radar data in the tropical tropopause region during NH spring and suggest that rapid uplift over land convective regions may be the dominant process of troposphere-to-stratosphere exchange. They suggest that the

ACPD
9, 25049–25084, 2009

maximum penetration of convective systems into the lower stratosphere would occur primarily over Africa at all seasons. Beginning in 2001, the large project AMMA (African Monsoon Multidisciplinary Analyses) was set up to study the West-African monsoon and its influence on the physical, chemical and biological environment, regionally and globally. The overall objective of the project was to provide the underpinning science that relates variability of the West African Monsoon to issues of health, water resources, food security and demography for West-African nations and to define and implement relevant monitoring and prediction strategies (www.amma-international.org). Within the frame of AMMA and the project SCOUT-O3 (Stratospheric-Climate Links with Emphasis on the Upper Troposphere and Lower Stratosphere) an aircraft campaign took place at the peak of the summer monsoon period in 2006, probing the air from the boundary layer up to the stratosphere (Cairo et al., 2009). The campaign took place in July/August 2006 and was based in Ouagadougou, Burkina Faso. The main aim of this aircraft campaign was to quantify the contribution of different air mass origins on the chemical composition of the TTL during the summer monsoon over West Africa. At this time of year the TTL can be impacted by recent local or regional convective uplift, but also by uplift from the lower troposphere upwind (e.g. over Asia), intrusion of air from the mid-latitude lower stratosphere or cross-hemispheric transport of air masses from the Southern Hemisphere (Law et al., 2009). A detailed description of the meteorological situation during the West-African monsoon in 2006 can be found in Janicot et al. (2008). In this paper we will present in situ tracer data of CO_2, N_2O, O_3 and CO that were obtained on board the M55 Geophysica aircraft during the AMMA/SCOUT-O3 project and analyse them regarding the principal transport processes that control the chemical composition of the TTL and tropical lower stratosphere above West-Africa. Vertical profiles and correlations between the various species, serving as stratospheric tracers, as boundary layer tracers, or age-of-air tracers will be used to contrast observations of the background TTL with convectively influenced air, to diagnose irreversible mixing of convectively overshooting air with the background TTL, and to assess isentropic mixing across the subtropical tropopause and the subtropical transport barrier.

ACPD
9, 25049–25084, 2009

2 In situ measurements

Tracer measurements were made between 31 July and 17 August 2005 on board the M55 Geophysica aircraft from (and during transfer to/from) Ouagadougou, Burkina Faso (12° N, 1° W). A total of nine flights were performed with measurements from the free troposphere up to the tropical lower stratosphere around 20 kilometer altitude. Four transfer flights were made between Verona (Italy), Marrakech (Morocco) and Ouagadougou (Burkina Faso). Five local flights between 4° N and 17° N latitude and 3° W and 3° E longitude were made to study mesoscale convective systems (MCS) and long range transport, and to validate the CALYPSO satellite. A brief overview of the flights is given in Table 1. A more extended overview of the flights and the Geophysica campaign can be found in Cairo et al. (2009). A suite of long-lived tracers (CO_2, N_2O, CFC−12, CFC−11, H−1211, SF_6, CH_4, H_2) was measured by the University of Frankfurt's High Altitude Gas Analyzer (HAGAR) on all flights except on 7 August when a software failure occurred. HAGAR is a two-channel in situ gas chromatograph (GC) that is combined with a CO_2 sensor (LI-COR 6251). The two GC-channels with electron capture detectors (ECD) measure the long-lived tracers N_2O, CFC−12, CFC−11,H−1211, CH_4, SF_6 and H_2 with a time resolution of 90 s. The CO_2 sensor achieves a time resolution of 5 s using non-dispersive infrared absorption (NDIR). A detailed description of the instrument can be found in Riediger (2000) and Strunk (1999). Frequent in flight calibrations within the instrument were performed in order to meet the specifications for accuracy and precision. All measurements are directly traceable to the current WMO scales based on intercalibrations against standards of NOAA/GMD or (for CO_2) the University of Heidelberg (I. Levin). For CO_2 the mean precision during all flights was 0.3 ppm. The precisions for the measurement of the other tracers are in the order of 0.5–3%; for the N_2O measurements used in this study it is better than 1.5%. Accuracies of the HAGAR measurements is limited by the precision and are thus only slightly larger than these precision values. Additionally, CO was measured with a precision of 1% and accuracy of 6–9% by the Italian institute

ACPD
9, 25049–25084, 2009

INOA (Istituto Nazionale di Ottica Applica) with the tunable diode laser COLD (Cryogenically Operated Laser Diode) as described in detail by Viciani et al. (2008). Ozone was measured with the Fast Ozone ANalyzer (FOZAN) of the Central Aerological Observatory (CAO, Russia) (Ulanovsky, 2001) with an accuracy of 10%. Mixing ratios for all gas measurements are expressed in dry mole fractions. Flight parameters as altitude, pressure and temperature were recorded by the aircraft.

3 Analysis of main transport processes

The results of the analysis of the different transport processes occurring in the summer TTL over West-Africa will be discussed in the following sections. Section 3.1 describes both main convective outflow as well as overshooting convection, Sect. 3.2 describes isentropic stratospheric inmixing across the subtropical tropopause and Sect. 3.3 describes isentropic mixing across the subtropical barrier in the lower stratosphere. Each section will have a short introduction about the concepts of the transport process described.

3.1 Convection

Convection plays an important role in determining the thermodynamic and chemical properties of the TTL. It can provide a fast pathway for halogenated very short lived species and other boundary layer trace gases to reach the TTL and subsequently the stratosphere, where they could contribute to the depletion of ozone. The amount of very short lived species that can reach the stratosphere thus depends crucially on the convective mass flux into the TTL as well as the maximum altitude level that is reached by deep convection. There are two mechanisms in which convection contributes to vertical transport through the TTL. The first is direct convective uplift to the level of neutral buoyancy, which is located at a potential temperature of at most 365 K (Folkins et al., 2000). At this level the potential temperature becomes equal to the highest

ACPD
9, 25049–25084, 2009

equivalent potential temperatures realized in the marine boundary layer. It is therefore near the maximum altitude an air parcel from the boundary layer can reach by undiluted, nonovershooting ascent (Reid and Gage, 1981). This convection up to the level of neutral buoyancy can be followed by slow diabatic ascent up to and across the tropopause due to radiative heating and the dynamical forcing by the Brewer Dobson circulation (Folkins et al., 1999). The typical time scales for this diabatic transport, as derived from numerical models and tracer measurements, range between 2 and 3 months for the upward transport from a potential temperature of 350 K up to 390 and 420 K, respectively (e.g., Andrews et al., 1999). The second mechanism, by which convection can influence the TTL to much higher levels than its neutral buoyancy level, is irreversible mixing of air following dynamic overshooting (Danielsen, 1982, 1993; Sherwood, 2000). When an air parcel overshoots its level of neutral buoyancy it will be colder than the surrounding air and start descending back to its equilibrium level. However, when it entrains and mixes with warmer surrounding air it will come to rest at a warmer, higher equilibrium level, i.e. its potential temperature increases (Danielsen, 1982). This overshooting of convection occurs predominantly above continental areas (Liu and Zipser, 2005; Zipser et al., 2006) and in large mesoscale convective systems (Rossow and Pearl, 2007), which are generated regularly over West-Africa in the monsoon period, thereby providing a fast pathway for boundary layer air into the upper TTL or even the lower stratosphere. Although the existence of this mechanism is generally accepted, its importance at global scale is less clear. In this section the two mechanisms for convective influence will be studied with help of the tracer data measured during AMMA/SCOUT-O3. In Sect. 3.1.1 we will examine the first mechanism and assess the level of main convective outflow and the influence of local and aged convection on the CO_2 profiles. In Sect. 3.1.2 we will examine the data for signatures of overshooting air.

ACPD
9, 25049–25084, 2009

3.1.1 Main convective outflow

CO_2 can be used as a tracer for continental convection because its mixing ratio is reduced in the boundary layer due to uptake by vegetation during daytime. Deep convection during the African Monsoon season peaks in the evening (Sultan et al., 2007) when boundary layer CO_2 is expected to be around its minimum. Convective transport of boundary layer air into the TTL during the Monsoon season therefore results in a layer of low CO_2 mixing ratios around the level of main convective outflow. Above this level, diabatic ascent is expected to dominate convection, vertical mixing and mixing of older air from mid-latitudes into the tropics. Hence, a coherent "tape recorder" signal due to the monotonic aging of the slowly ascending air and the progressing CO_2 seasonal cycle in the tropospheric boundary layer can be observed (Boering et al., 1996; Park et al., 2007). In this section we will discuss the strength and height of the main convective influence with help of the CO_2 profiles and compare with results of an analysis by Law et al. (2009). Law et al. (2009) calculate the fraction of measured air that has potentially been influenced by recent convection with help of ECMWF backtrajectories and infrared satellite images identifying convective clouds. They label an airmass as possibly recently convectively influenced when its backward trajectory crossed a region whose cloud top radiance was below 200 K within a longitudinal band from 30° W to 40° E, corresponding to an age of at most three to four days. Figure 1 shows the vertical CO_2 profiles for the four local flights on 4, 8, 11 and 13 August, respectively. Mixing ratios as low as 372 ppm are observed in the daytime boundary layer over Ouagadougou; even lower values could be present in rural areas. The influence of vegetative uptake of CO_2 is getting smaller in the free troposphere, resulting in higher mixing ratios of around 380 ppm. Convection during afternoon and evening transports the CO_2-depleted boundary layer air up to about 13–14 km, or a potential temperature level of 350 K (Fig. 2), where again a distinct layer with low mixing ratios is observed. Above this level the typical coherent "tape recorder" signal is observed. The flight of 11 August shows the highest and strongest outflow signature, with mixing

ACPD
9, 25049–25084, 2009

ratios as low as 374 ppm found up to 370 K. This flight aimed specifically at sampling air influenced by a large and intense MCS that had crossed westward across Burkina Faso during the previous days (Cairo et al., 2009). Law et al. (2009) also find that of all flights performed during the campaign, the TTL sampled during the flight on 11 August was most influenced by recent convection. They calculate that for this flight 7–10% of the measured air between 340 and 380 K was possibly influenced by recent convective activity. Our CO_2 observations suggest that convective outflow of this intense MCS in fact reached unusually high potential temperatures of 370 K. For the flight of 8 August, Law et al. (2009) also indicate possible convective influence up to a level of 390 K, although to a lesser extent, i.e. for only 2 to 5% of the measured air. This agrees well with the CO_2 profile, which shows a level of main convective outflow at 350 K with a CO_2 mimimum that is less pronounced than on 11 August. However, above this level the "tape recorder" signal is less compact as during the other flights, which might be an indication of overshooting convection, which will be discussed in the next section. For the flight of 4 August, the CO_2 profile shows again a recognizable level of main convective outflow at 355 K, again less distinct as for the flight of 11 August. Law et al. (2009) indeed infer possible influence of recent convection for only 3 to 4% of the air, and just up to 355 K, during that day. Least influence of convection is evident in the profile of 13 August, where an outflow level can hardly be discerned, with mixing ratios at 13 km as high as in the free troposphere. This again agrees well with the analysis of Law et al. (2009), who also find least possible influence of recent convection (less than 2% above 350 K) during this flight. Overall, the observed features in the CO_2 profiles and their relative strengths and maximum altitudes are thus qualitatively in line with the fractions of sampled air having recently (within about 4 days) passed over convective systems, as calculated by Law et al. (2009). However, these fractions are calculated to be on the order of a few percent only (at most 10% for 11 August). The observed pronounced CO_2 reductions by up to 4 ppm in the convective outflow region cannot easily be explained by such small recent convective input, unless regional boundary layer mixing ratios are much lower on the average than those actually

ACPD
9, 25049–25084, 2009

observed over Ouagadougou. Another, more likely, explanation is that the CO_2minima are not only due to recent convection, but to a larger part caused by older convection having occured more than four days ago. Since CO_2 is chemically conserved in the TTL, it is not possible to distinguish between the effects of recent and older convection with help of the CO_2 profiles. However O_3 profiles can give an indication whether the convection was of recent or of older origin. In the tropical boundary layer typical ozone mixing ratios range from 15 to 40 ppb (Folkins and Martin, 2005). Deep convection will transport this O_3 poor air together with ozone precursors from the tropical boundary layer into the TTL, where, as long as no new convective input takes place, the mixing ratio will steadily increase by photochemical production until it reaches its steady state. Therefore, O_3 mixing ratios are an indication for the convective replacement timescale over a region. However, not only convection, photochemical production, and the time since the air has last experienced convective flushing determine the O_3 mixing ratios in the TTL. The O_3 budget in the TTL can also be significantly affected by isentropic stratospheric inmixing bringing in extratropical stratospheric air with high O_3 mixing ratios. Vertical mixing, e.g. following overshooting of air, may also mix down higher ozone concentrations from higher altitudes. We show in Sect. 3.2 that horizontal stratospheric inmixing, however, is not significant during the four flights considered here. Mixing following overshooting will be discussed in the next section (Sect. 3.1.2). Figure 3 shows the ozone profiles during the AMMA campaign. The average profile of all five local flights is indicated as the black line. For comparison, the dark green line represents the average ozone profiles during the SCOUT-O3 campaign, which took place in November and December 2005 above northern Australia. This latter profile shows the typical S-shape, with low O_3 mixing ratios of 30 ppb over the marine boundary layer, increasing concentrations in the free troposphere, again low O_3 mixing ratios at the level of main convective outflow, and above that increasing mixing ratios due to the photochemical production of O_3 in the lower stratosphere. The AMMA-SCOUT-O3 profiles also show this S-shape profile, although less pronounced. Again, concentrations are average to about 30 ppb in the boundary layer; this mean value above Ouagadougou agrees also

ACPD
9, 25049–25084, 2009

well with that observed in the boundary layer over Niamey, Niger, by regularly launched ozone sondes (Cairo et al., 2009) and is thus thought to be fairly representative for a wider region. In the free troposphere O_3 increases with height up to around 60 ppb at a potential temperature level of 340 K. O_3 mixing ratios at the level of main convective outflow, however, are much higher on average than those observed during the SCOUT-O3 campaign or in the boundary layer during AMMA-SCOUT-O3. For most of the flights no boundary layer values are observed at the main level of convective outflow (355 K), thereby indicating that recent convection had only a minor impact on the sampled air. Only on 4 August there are values as low as 30 ppb found at a level of 355 K, indicating more recent convective flushing. Above 370 K the O_3 mixing ratios are up to twice as high as during the SCOUT-O3 campaign. Randel et al. (2007) show that in a narrow vertical layer between ~16 and 19 km (~375–450 K) approximately a factor 2 change in ozone between the minimum (during NH winter) and maximum (during NH summer) takes place due to variations in vertical transport associated with mean upwelling in the lower stratosphere (the Brewer Dobson circulation). Folkins et al. (2006) show with help of ozone sondes that the seasonal difference in upwelling can explain 20 to 40 ppb of the difference between August and November/December at the 370 K level. Thus, the higher mixing ratios observed during AMMA are probably caused by the seasonal difference in upwelling due to the Brewer Dobson circulation. In summary, the CO_2 profiles show that the region around West-Africa is highly influenced by convection up to 355 K, during 11 August even up to 370 K. Clearly pronounced levels of main convective outflow are observed during three of the four flights. However, O_3 profiles strongly suggest that this convective influence is mostly of older origin, and has been transported for at least several days before measured. Only the observations of 4 August exhibit some signatures of recent convection in the O_3 profile. Overall, these results are in good agreement with the findings of Law et al. (2009).

3.1.2 Overshooting of convection

Now we examine potential signatures of overshooting convection in the tracer data by observations of CO, CO_2 and O_3. In Fig. 4 the CO_2 profiles during AMMA/SCOUT-O3 are plotted in one figure, with their average represented by the black line. On 8 August there are large deviations from this average between 390 and 420 K. Both enhanced and reduced values of CO_2 can be found at this level. On 4 August there are also some reduced values between 400 and 420 K. The enhanced values on 8 August cannot be explained by transport processes; given they occur shortly after a calibration phase of the instrument we cannot completely rule out an unusual instrumental instability. The low values could be an indication of irreversible mixing of overshooting air. If irreversible mixing takes place during or following convective overshoot, air parcels originating from the boundary layer with a potential temperature of 350–360 K (the level of neutral buoyancy) will mix with air masses with a higher potential temperature along a mixing line. In practice, mixing may proceed along a multitude of such mixing lines resulting in a mixing band in a profile plot (provided sufficient sampling). In Fig. 4, two possible idealized mixing lines are displayed. They indicate that, in order to explain the signatures, mixing would have occurred between air parcels with potential temperatures of approximately 355 K and 400–420 K, that is overshooting convection would have reached up to 17–18 km. Overshooting convection can also be diagnosed in tracer-tracer correlations. Without mixing, the correlation between a tropospheric (e.g. CO, CO_2) and a stratospheric tracer (e.g. O_3) will form an L-shape: in the troposphere an almost constant mixing ratio of the stratospheric tracer and much variation in the mixing ratio of the tropospheric tracer, and the opposite in the upper TTL and stratosphere. Thus, the correlation plot exhibits two distinct branches for the stratosphere and the tropopsphere, which meet in the lower TTL. Mixing following overshooting would again be seen along mixing lines between these two branches, connecting boundary layer observations with values observed at the highest level of overshoot. Figure 5 shows the correlation plot between O_3 and CO_2 for the local flights, coloured according to potential temperatures

ACPD
9, 25049–25084, 2009

and with the average correlation in black. The figure shows a flipped L-shape with variable CO_2 mixing ratios and constant O_3 mixing ratios in the troposphere up to about 360 K, and above that increasing O_3 mixing ratios and slowly decreasing CO_2 mixing ratios. Again, the correlation plot shows a deviation from the average correlation curve between potential temperatures of about 360 and 420 K. They occur along mixing lines corresponding to those displayed in Fig. 4. However, similar signatures are not observed during that part of the flight in other species like H_2O, NO_y and particles (not shown). If overshooting of convection had occurred one would expect clear signals of enhanced H_2O and particles as moister air with more particles from the boundary layer would be entrained. Voigt et al. (2008) indicate layers with enhanced particles and NO_y, but these are found at other locations during the flight. The latter study does, however, show with backtrajectories that the air measured during this flight was located above a mesoscale convective system for at least 1.5 days prior to the measurements, with cloud top levels up to at least 120 hPa (16 km altitude). As during the flight of 7 August CO_2 was not measured due to failure of the HAGAR instrument we examine the CO data measured by the COLD instrument. Figure 6 shows the CO profiles for both 7 and 8 August (the only flights during which COLD measured). Around 410 K, very high CO mixing ratios are observed, which could again be an indication of vertical mixing following overshooting. This feature is also present in the correlation plot between CO and O_3, which is shown in Law et al. (2009). However, as the two possible mixing lines in Fig. 6 indicate, this would imply mixing of air from the main convective outflow level (355 K) with air parcels at potential temperatures of at least 430 K, i.e. overshoot to extremely high levels. Again, other tracers do not show similar signatures. Although enhancements are observed in mixing ratios of NO_y and CCN during that day, these only indicate an influence up to 14–15 km, and during a later section of the flight (not shown). Water vapour mixing ratios do not show any signatures indicative of overshooting convection (not shown). Overall, we conclude that signatures potentially indicating impact of overshooting convection are observed in the lower stratosphere in the CO and CO_2 mixing ratios during the AMMA campaign. However,

these signatures are not corroborated by measurements from other instruments on board the airplane. Thus, evidence for the impact of overshooting is inconclusive. In particular, there is no clear indication that overshooting of convection plays a major role in troposphere-to-stratosphere transport during the time of the campaign.

3.2 Stratospheric isentropic inmixing into the TTL

Horizontally, the tropical tropopause layer is confined by the subtropical jets. The strength and position of these jets vary by season, with a strong jet close to the equator in the winter hemisphere and a weak, poleward shifted jet in the summer hemisphere. Haynes and Shuckburgh (2000) show that a strong subtropical jet forms an effective transport barrier for the meridional, isentropic transport between the lower part of the TTL and the extratropical lower stratosphere.

Isentropic, quasi-horizontal transport from the extra-tropical stratosphere may play a significant role in determining the chemical (trace species) and radiative character of the TTL (Gettelman and Forster, 2002). Analysis of previous aircraft measurements suggests that there may be significant quasi-isentropic transport from the lower mid-latitude stratosphere toward the tropics (Tuck et al., 2003; Marcy et al., 2007). In order to quantify the amount of extratropical stratospheric air entering the TTL we examine the N_2O data. N_2O has its source located at the surface and is well mixed throughout the troposhere. Photochemical sinks in the mid-stratosphere result in declining N_2O mixing ratios above the tropopause. Reductions in N_2O mixing ratios below the typical tropospheric value therefore indicate entrainment of stratospheric, photochemically aged (in the order of years) air masses. The profiles of N_2O shown in Fig. 7 exhibit constant tropospheric concentrations for the local flights, and a well defined decrease from the tropopause upward, indicating that mixing with stratospherical older air masses is exceedingly rare below the tropopause, whereas the decrease just above the tropopause indicates increasing in-mixing of older air masses. The measurements made in Verona and during the transfer flights ($> 30^{\circ}$ N) show decreasing N_2O values above 330 K, indicating the level of the tropopause in the extratropical region. In order

ACPD
9, 25049–25084, 2009

to estimate the fraction of air transported from the extratropical lower stratosphere the N_2O mixing ratios of the extratropical stratosphere are compared with the values in the TTL. The fraction of aged extratropical air (χ) can be expressed as:

$$\chi = \frac{[N_2O] - [N_2O]_{trop}}{[N_2O]_{extratrop} - [N_2O]_{trop}}, \quad (1)$$

where $[N_2O]$ is the measured N_2O mixing ratio; $[N_2O]_{trop}$ is the average N_2O mixing ratio at the bottom of the TTL, inferred as the average between potential temperatures of 320 K and 350 K between 0–20° N; $[N_2O]_{extratrop}$ is the average N_2O mixing ratio of the extratropical lowermost stratosphere, inferred as the average between potential temperatures of 350 K and 400 K during all flights northward of 40°. The values derived here are $[N_2O]_{extratrop}$=309 and $[N_2O]_{trop}$=320 ppb. Fig. 8 shows the derived fraction of extratropical air in the TTL. The blue line represents the average height of the cold point tropopause during the campaign. The fraction of aged extratropical air in the TTL is around zero in the lower part up to 370 K and is only slightly increasing towards the top of the TTL (here defined as the cold point tropopause). Note that this result refers to in-mixing of photochemically aged air only and thus does not necessarily rule out in-mixing of extra-tropical stratospheric air altogether. In fact active isentropic exchange across the weak summer subtropical jet with a net export of air masses from the TTL to the extratropical stratosphere is known to flush the lowermost stratosphere with young air over the course of the summer. Any re-entrainment of these young air masses into the TTL would not be detected by the above diagnostic (but would also be of little relevance for the chemical composition of the TTL).

3.3 Isentropic mixing across the subtropical barrier

Except for its lowest part where isentropic mixing with the extratropics is still relatively efficient, the tropical stratosphere is more or less isolated from the extratropical part of the stratosphere (Volk et al., 1996; Minschwaner et al., 1996). The subtropical barrier constitutes a region of strong horizontal shear and maximum PV gradient along

isentropes, thereby prohibiting fast isentropic mixing between the tropical stratosphere and mid-latitude stratosphere, especially in the winter hemisphere. Due to the isolation of the tropical stratosphere, tracer pairs with differing source/sink structures (e.g. O_3–N_2O, O_3–NO_y) show different correlation slopes in the tropical and extratropical stratosphere (Volk et al., 1996; Fahey et al., 1996). At mid-latitudes, where quasi-horizontal mixing is faster than both vertical transport and chemical time scales, a compact correlation evolves whose slope at any point is determined by the ratio of globally integrated sources and sinks of the two species above the given altitude (Plumb and Ko, 1992). Further, since the sources and sinks for O_3 and N_2O are insignificant in the lower stratosphere, this ratio remains approximately constant there, and thus the lower stratospheric correlation is fairly linear. In the tropics, on the other hand, quasi-horizontal mixing is slower, and the correlation is to a large part determined by vertical ascent and local chemistry (Volk et al., 1996); in situ production of O_3 in the lower stratosphere thus results in a correlation slope different from the mid-latitudes. The correlation slope is thus a reliable indicator for the origin of an air mass. A change in the slope of these correlation branches marks the position of the subtropical barrier. Mixing events between the two regions manifest themselves as lines or bands connecting the characteristic tropical and extratropical correlation branches. Figure 9 shows the correlation between O_3 and N_2O for the local and the transfer flights during AMMA/SCOUT-O3. The colours indicate the latitude of the measurements. Different correlation slopes are observed at different latitudes. The slopes of these correlations are visualised in Fig. 10 by plotting the ratio of the differences between the measured O_3 and N_2O values from tropospheric reference values, i.e. plotting the correlation slope from the tropospheric origin of the correlation (chosen as 320 ppb N_2O and 50 ppb O_3). The figure shows only data above a potential temperature of 415 K, above which a significant separation between the tropical and midlatitude correlations can be discerned. The lowest slope values of 0.02 observed southward of 15° N indicate air within the isolated tropical region (the "tropical pipe"), whereas the midlatitudes exhibit slope values exceeding 0.04. Values in between these extremes are found in a

band between 10° N and 30° N, suggesting a wider transition zone rather than a sharp subtropical barrier. In order to examine whether the subtropical barrier might nevertheless be sharp, but undulate within that latitude band due to wave motions, we also plot the slope values against equivalent latitude in Fig. 11. Reversible wave motions should be mostly eliminated in this projection as they occur at roughly conserved potential vorticity, and thus equivalent latitude. Nevertheless, the transition between inner tropical and midlatitude slope values still spans a band between 10° N and 25° N equivalent latitude. It thus appears that during AMMA there is not a sharp barrier but a subtropical transition zone with a width of about 15° latitude. In Fig. 12 we compare our results with correlation slopes (N_2O vs O_3) found earlier during the ASHOE/MAESA campaign in March and October/November 1994. The slope values from AMMA data are coloured and plotted against latitude. The ASHOE/MAESA slopes (in grey) can be viewed in analogy to the NO_y/O_3 ratios published in (Fahey et al., 1996) and in fact show fairly sharp transitions between low tropical values and extratropical values in March (around 10° N) and in October (around 15° N). In contrast, the transition during AMMA in August is more gradual and ranges between 10° N and 25° N. We note here that the ER-2 data from ASHOE/MAESA in the region in question are on average sampled at a higher altitude than the M55 data from AMMA, the former being mostly collected during transfer flights at maximum altitude (20–21 km). As the subtropical barrier increases in strength above 20 km, the ASHOE/MAESA data are thus expected to be more suitable to indicate the location and width of the barrier, whereas the Geophysica during AMMA may have sampled at an altitude range (below 20 km) at which the barrier is weaker and thus more permeable to mixing. On the other hand, the subtropical barrier is also expected to be weakest during summer on the summer hemisphere due to the absence of strong wave activity in the surf zone, which tends to shapen the barrier. Thus the observed differences between ASHOE/MAESA and AMMA in the width of the transition between tropical and extratropical tracer values may well be explained by differences in both sampling altitude and season.

ACPD
9, 25049–25084, 2009

4 Conclusions

We have presented in situ tracer data from the AMMA-SCOUT-O3 campaign in July/August 2006 over West-Africa. Data were obtained on board the M55 Geophysica with the High Altitude Gas ANalyzer (HAGAR), measuring CO_2, N_2O, CFC−11, CFC−12, H−1211, CH_4, SF_6 and H_2, as well as from the FOZAN and COLD instruments, measuring O_3 and CO, respectively. We have used the data to examine the dominant transport processes in the TTL: deep convection up to the level of main convective outflow, irreversible mixing after overshooting of deep convection, isentropic inmixing into the TTL across the subtropical tropopause, and horizontal transport in the region of the subtropical barrier. The CO_2 profiles (with the exception of 13 August) show distinct minima in the TTL, reflecting the outflow of boundary layer air depleted in CO_2. These reductions in CO_2 suggest that i) convective influence in the TTL is quite significant in the sampled air masses and that ii) the main convective outflow was usually located at potential temperature levels up to ~350–360 K (13–14 km), and for the flight of 11 August even reached up to 370 K (~15 km). The O_3 profiles, on the other hand, indicate that the larger part of the convective fraction in the sampled air masses must be of rather older origin (several days), as regional boundary layer mixing ratios of 30 ppb are only occasionally found in the TTL (only during the flight of 4 August), while average O_3 mixing ratios in the TTL are observed to be 50 ppb or higher. Overshooting convection does not seem to have a large impact on vertical profiles of tracers, which exhibit quite coherent shapes above the maximum level of convective outflow. Only a few small signatures potentially indicative of mixing following overshooting convection were observed in the CO_2 data during the flights of 4 and 8 August; another potential signature was observed in CO on 7 August. However, similar signatures were not simultaneously observed in other tracers. Stratospheric inmixing of photochemically aged air from the extratropical stratosphere appears to be minimal up to the mean local tropopause at 376 K. The fractions of aged extratropical air in the TTL, as estimated from N_2O profiles is 0.0±0.1 up to 370 K and is increasing above this level up to a about

ACPD
9, 25049–25084, 2009

(0.2±0.13) at 390 K. The subtropical barrier does not manifest itself as a sharp boundary in tracer distrubutions, but rather as a gradual transition region between around 10 and 25° N where tracer mixing ratios change from characteristic tropical to extratropical values. The subtropical barrier thus appears to be rather permeable to horizontal mixing in the summer subtropics below 20 km altitude.

Acknowledgements. This research was supported by the European Community under the Integrated Project SCOUT-O3 (505390-GOCE-CT-2004) as well as by the AMMA-EU project. Based on a French initiative, AMMA was built by an international scientific group and is currently funded by a large number of agencies, especially from France, UK, US and Africa. It has been the beneficiary of a major financial contribution from the European Community's Sixth Framework Research Programme. Detailed information on scientific coordination and funding is available on the AMMA International web site http://www.amma-international.org. We also would like to thank the pilot and the crew of the M55 Geophysica and our colleagues who made the AMMA-SCOUT-O3 campaign a success. Finally we are grateful to Horst Fischer for support with the implementation of the Licor CO_2 sensor within the HAGAR instrument.

References

AMMA Public: http://www.amma-international.org/rubrique.php3?id_rubrique=1, last access: 25 May 2009.

Andrews, A. E., Boering, K. A., Daube, B. C., Wofsy, S. C., Hintsa, E. J., Weinstock, E. M., and Bui, T. P.: Empirical age spectra for the lower tropical stratosphere from in situ observations of CO2: Implications for stratospheric transport, J. Geophys. Res., 104(D21), 26581-26596, 1999. 25056

Boering, K. A., Wofsy, S. C., Daube, B. C., Schneider, H. R., Loewenstein, M., and Podolske, J. R.: Stratospheric mean ages and transport rates from observations of carbon dioxide and nitrous oxide, Science, 274(5291), 1340-1343, 1996. 25057

Cairo, F., Pommereau, J. P., Law, K. S., Schlager, H., Garnier, A., Fierli, F., Ern, M., Streibel, M., Arabas, S., Borrmann, S., Berthelier, J. J., Blom, C., Christensen, T., D'Amato, F., Di Donfrancesco, G., Deshler, T., Diedhiou, A., Durry, G., Engelsen, O., Goutail, F., Harris, N. R. P., Kerstel, E. R. T., Khaykin, S., Konopka, P., Kylling, A., Larsen, N., Lebel, T., Liu, X.,

MacKenzie, A. R., Nielsen, J., Oulanowski, A., Parker, D. J., Pelon, J., Polcher, J., Pyle, J. A., Ravegnani, F., Rivière, E. D., Robinson, A. D., Röckmann, T., Schiller, C., Simões, F., Stefanutti, L., Stroh, F., Some, L., Siegmund, P., Sitnikov, N., Vernier, J. P., Volk, C. M., Voigt, C., von Hobe, M., Viciani, S., and Yushkov, V.: An overview of the SCOUT-AMMA stratospheric aircraft, balloons and sondes campaign in West Africa, August 2006: rationale, roadmap and highlights, Atmos. Chem. Phys. Discuss., 9, 19713–19781, 2009, http://www.atmos-chem-phys-discuss.net/9/19713/2009/. 25053, 25054, 25058, 25060

Danielsen, E. F.: A dehydration mechanism for the stratosphere, Geophys. Res. Lett., 9(6), 605–608, 1982. 25056

Danielsen, E. F.: In situ evidence of rapid, vertical, irreversible transport of lower tropospheric air into the lower tropical stratosphere by convective cloud turrets and by larger-scale upwelling in tropical cyclones, J. Geophys. Res., 98, 8665-8681, 1993. 25056

Fahey, D. W., Donelly, S. G., Keim, E. R., Gao, R. S., Wamsley, R. C., Del Negro, L. A., Woodbridge, E. L., Proffitt, M. H., Rosenlof, K. H., Ko, M. K. W., Weisenstein, D. K., Scott, C. J., Nevison, C., Solomon, S., and Chan, K. R.: In situ observations of NO_y, O_3 and the NO_y/O_3 ratio in the lower stratosphere, Geophys. Res. Lett., 23, 1653–1656, 1996. 25065, 25066

Folkins, I., Oltmans, S. J., and Thompson, A. M.: Tropical convective outflow and near surface equivalent potential temperatures, Geophys. Res. Lett., 27, 2549–2552, 2000. 25055

Folkins, I., Bernath, P., Boone, C., Lesins, G., Livesey, N., Thompson, A. M., Walker, K., and Witte, J. C.: Seasonal cycles of O3, CO, and convective outflow at the tropical tropopause, Geophys. Res. Lett., 33, L16802, doi:10.1029/2006GL026602, 2006. 25060

Folkins, I., Loewenstein, M., Podolske, J., Oltmans, S. J. and Profitt, M.: A barrier to vertical mixing at 14 km in the tropics: Evidences from ozonesondes and aircraft measurements, J. Geophys. Res., 104, 22095–22102, 1999. 25056

Folkins, I. and Martin, R. V.: The vertical structure of tropical convection and its impact on the budgets of water vapor and ozone, J. Atmos. Sci., 62, 1560–1573, 2005. 25059

Gettelman, A. and Forster, P. M.: A climatology of the tropical tropopause layer, J. Meteorol. Soc. Japan, 80, 911–924, 2002. 25051

Hoor, P., Fischer, H., Lange, L., Lelieveld, J., Brunner, D.: Seasonal variations of a mixing layer in the lowermost stratosphere as identified by the CO-O3 correlation from in situ measurements, J. Geophys. Res., 107(D5), 4044, doi:10.1029/2000JD000289, 2002. 25052

Janicot, S., Thorncroft, C. D., Ali, A., Asencio, N., Berry, G., Bock, O., Bourles, B., Caniaux,

G., Chauvin, F., Deme, A., Kergoat, L., Lafore, J.-P., Lavaysse, C., Lebel, T., Marticorena, B., Mounier, F., Nedelec, P., Redelsperger, J.-L., Ravegnani, F., Reeves, C. E., Roca, R., de Rosnay, P., Schlager, H., Sultan, B., Tomasini, M., Ulanovsky, A., and ACMAD forecasters team: Large-scale overview of the summer monsoon over West Africa during the AMMA field experiment in 2006, Ann. Geophys., 26, 2569–2595, 2008, http://www.ann-geophys.net/26/2569/2008/. 25053

Law, K., Cairo, F., Fierli, F., and others: Air mass origins influencing TTL chemical composition over West Africa during the summer monsoon, 2009. 25053, 25057, 25058, 25060, 25062

Liu, C. and Zipser, E. J.: Global distribution of convection penetrating the tropical tropopause, J. Geophys. Res., 110, D23104, doi:10.1029/2005JD006063, 2005. 25056

Marcy T. P., Popp, P. J., Gao, R. S., Fahey, D. W., Ray, E. A., Richard, E. C., Thompson, T. L., Atlas, E. L., Loewenstein, M., Wofsy, S. C., Park, S., Weinstock, E. M., Swartz, W. H., and Mahoney, M. J.: Measurements of trace gases in the tropical tropopause layer, Atmos. Environ., 41, 7253–7261, doi:10.1016/j.atmosenv.2007.05.032, 2007. 25052, 25063

Minschwaner, K., Dessler, A. E., Elkins, J. W., Volk, C. M., Fahey, D. W., Loewenstein, M., Podolske, J. R., Roche, A. E., and Chan, K. R.: Bulk properties of isentropic mixing into the tropics in the lower stratosphere, J. Geophys. Res., 101, 9433–9439, 1996. 25064

Park, S., Jiménez, R., Daube, B. C., Pfister, L., Conway, T. J., Gottlieb, E. W., Chow, V. Y., Curran, D. J., Matross, D. M., Bright, A., Atlas, E. L., Bui, T. P., Gao, R.-S., Twohy, C. H., and Wofsy, S. C.: The CO_2 tracer clock for the Tropical Tropopause Layer, Atmos. Chem. Phys., 7, 3989–4000, 2007, http://www.atmos-chem-phys.net/7/3989/2007/. 25051, 25052, 25057

Plumb, R. A. and Ko, M. K. W.: Interrelationships between mixing ratios of long-lived stratospheric constituents, J. Geophys. Res., 97, 10145-10156,1992. 25051, 25065

Randel, W. J., Park, M., Wu, F., and Liveseya, N.: A large annual cycle in ozone above the tropical tropopause linked to the BrewerDobson Circulation, J. Atmos. Sci., 64, 4479–4488, doi:10.1175/2007JAS2409.1, 2007. 25060

Reid, G. C. and Gage, K. S.: On the annual variation in the height of the tropical tropopause, J. Atmos. Sci., 38, 1928–1938, 1981. 25056

Ricaud, P., Barret, B., Attié, J.-L., Motte, E., Le Flochmoën, E., Teyssèdre, H., Peuch, V.-H., Livesey, N., Lambert, A., and Pommereau, J.-P.: Impact of land convection on troposphere-stratosphere exchange in the tropics, Atmos. Chem. Phys., 7, 5639–5657, 2007, http://www.atmos-chem-phys.net/7/5639/2007/. 25052

Riediger, O.: Entwicklung und Einsatz eines flugzeuggetragenen Instrumentes zur in-situ-Messung langlebiger Spurengase in der Stratosphre, Ph.D. thesis, Johann Wolfgang Goethe Universität Frankfurt, Germany, 195 pp., 2000. 25054

Rossow, W. B. and Pearl, C.: 22-Year survey of tropical convection penetrating into the lower stratosphere, Geophys. Res. Lett., 34, L04803, doi:10.1029/2006GL028635, 2007. 25056

Sherwood, S. C.: A "stratospheric drain" over the maritime continent, Geophys. Res. Lett., 27, 677–680, 2000. 25056

Strunk, M.: An Experimental Study on the Mean Age of Stratospheric Air, Ph.D. thesis, Johann Wolfgang Goethe-Universität Frankfurt, Germany, 1999. 25054

Sultan, B., Janicot, S., and Drobinski, P.: Characterization of the Diurnal Cycle of the West African Monsoon around the Monsoon Onset, J. Climate, 20, 4014–4032, 2007.

Tuck, A. F., Hovde, S. J., Kelly, K. K., Mahoney, M. J., Proffitt, M. H., Richard, E. C. and Thompson, T. L.: Exchange between the upper tropical troposphere and the lower stratosphere studied with aircraft observations, J. Geophys. Res., 108(D23), 4734, doi:10.1029/2003JD003399, 2003. 25052, 25063

Ulanosvky, A. E., Yushkov, V. A., Sitnikov, N. M., and Ravegnani, F.: The FOZAN-II Fast-Response Chemiluminescent Airborne Ozone Analyzer, Instrum. Exp. Tech., 44(2), 249–256, 2001. 25055

Viciani, S., D'Amato, F., Mazzinghi, P., Castagnoli, F., Toci, G., and Werle, P.: A cryogenically operated laser diode spectrometer for airborne measurement of stratospheric trace gases, Appl. Phys. B, 90, 581–592, doi:10.1007/s00340-007-2885-2, 2008. 25055

Voigt, C., Schlager, H., Roiger, A., Stenke, A., de Reus, M., Borrmann, S., Jensen, E., Schiller, C., Konopka, P., and Sitnikov, N.: Detection of reactive nitrogen containing particles in the tropopause region - evidence for a tropical nitric acid trihydrate (NAT) belt, Atmos. Chem. Phys., 8, 7421–7430, 2008, http://www.atmos-chem-phys.net/8/7421/2008/. 25062

Volk, C. M., Elkins, J. W., Fahey, D. W., Salawitch, R. J., Dutton, G. S., Gilligan, J. M., Proffitt, M. H., Loewenstein, M., Podolske, J. R., Minschwaner, K., Margitan, J. J., and Chan, K. R.: Quantifying transport between the tropical and mid-latitude lower stratosphere, Science, 272, 1763–1768, 1996. 25052, 25064, 25065

Zipser, E. J., Cecil, D. J., Liu, C. T., Nesbitt, S. W., and Yorti, D. P.: Where are the most intense thunderstorms on earth?, B. Am. Meteorol. Soc., 87(8), 1057–1071, 2006. 25056

Table 1. Overview of flights during AMMA-SCOUT-O3.

Date of flight	Time (UTC)	Goal
31 07 2006	05:50–09:13	Transfer flight-UTLS profile
01 08 2006	10:59–14:59	Transfer flight-UTLS profile
04 08 2006	08:26–12:13	Long range transport
07 08 2006	12:15–16:07	MCS close up
08 08 2006	11:46–15:31	CALIPSO validation
11 08 2006	14:44–18:22	MCS aged outflow
13 08 2006	12:50–16:23	Long range transport
16 08 2006	13:27–15:16	Transfer flight-UTLS profile
17 08 2006	04:10–07:51	Transfer flight-UTLS profile

ACPD
9, 25049–25084, 2009

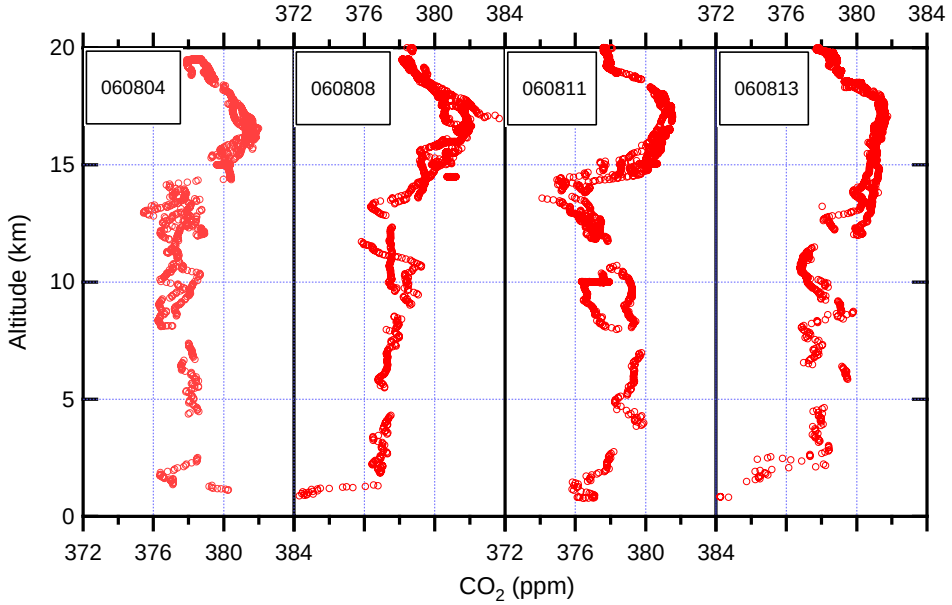

Fig. 1. Vertical profiles of CO_2 for the local flights on 4, 8, 11 and 13 August, respectively.

ACPD

9, 25049–25084, 2009

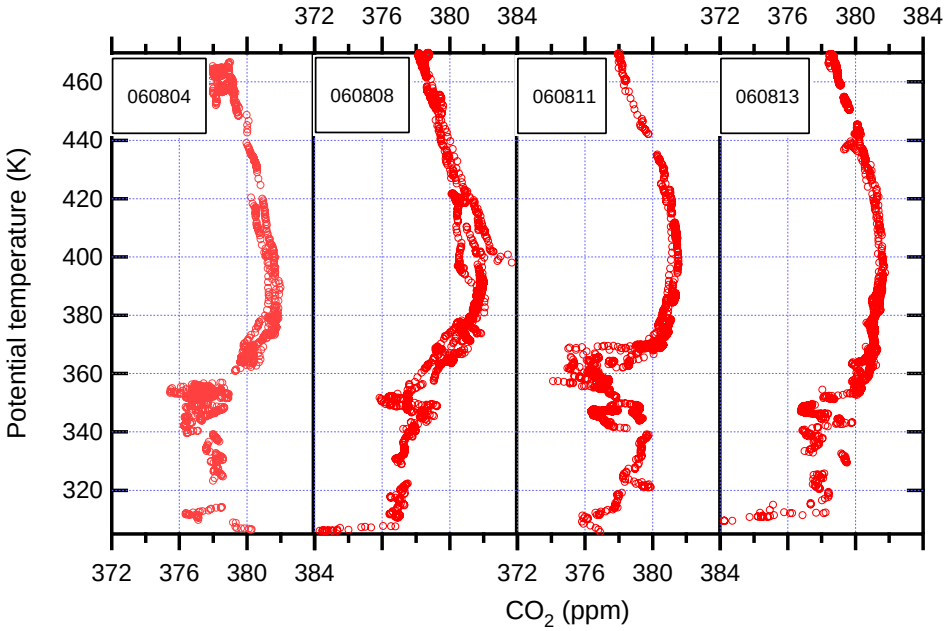

Fig. 2. Potential temperature profiles of CO_2 for the flights on 4, 8, 11 and 13 August, respectively.

ACPD
9, 25049–25084, 2009

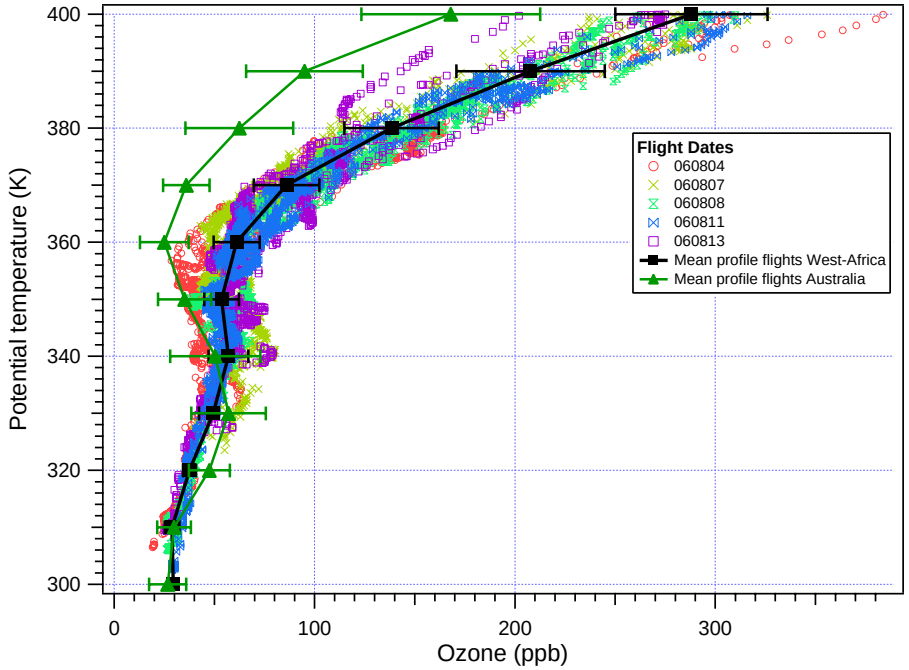

Fig. 3. Ozone profiles for the five local flights. The average profiles is indicated with the black line. The green line represents the average ozone profile for the SCOUT-O3 campaign over Australia in November/December 2005.

ACPD
9, 25049–25084, 2009

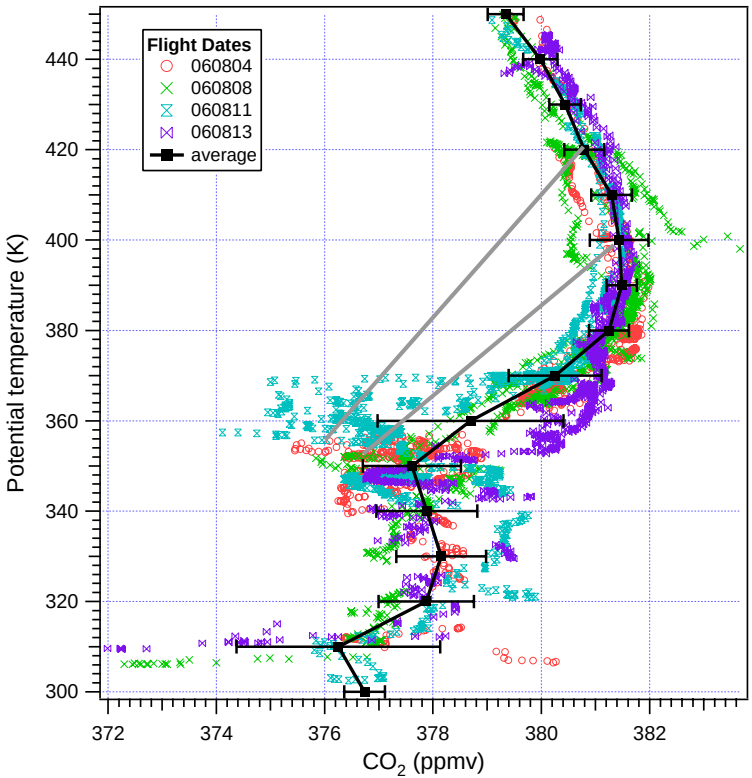

Fig. 4. CO_2 profiles for the local flights during AMMA/SCOUT-O3. Average profile in black. Two examples of possible mixing lines are presented by the grey lines

ACPD

9, 25049–25084, 2009

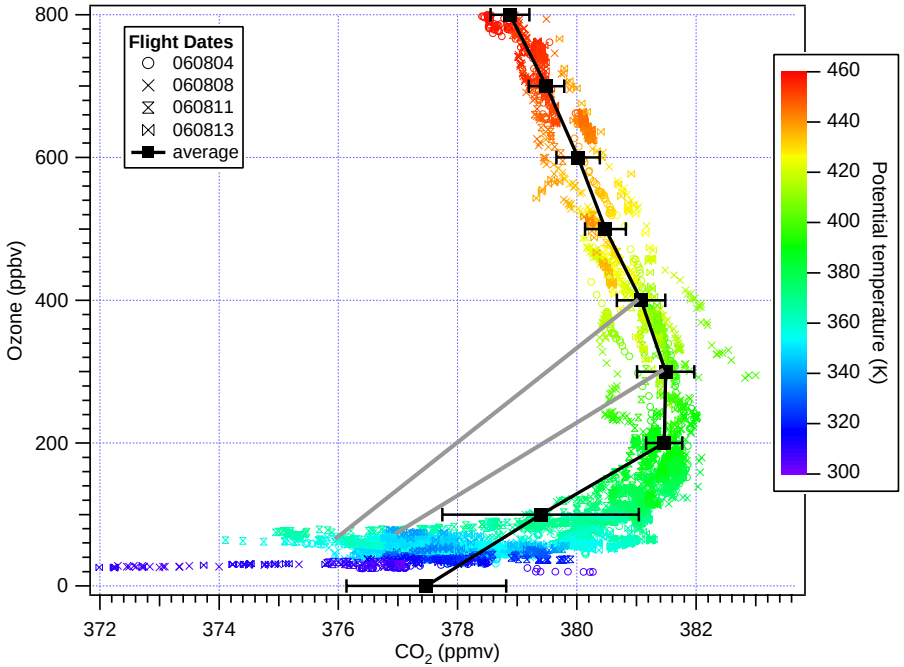

Fig. 5. Correlation between O_3 and CO_2. The data are coloured to potential temperature. The black line represents the average CO_2 profile for all local flights. The grey lines are the possible mixing lines that are also displayed in Fig. 4.

ACPD
9, 25049–25084, 2009

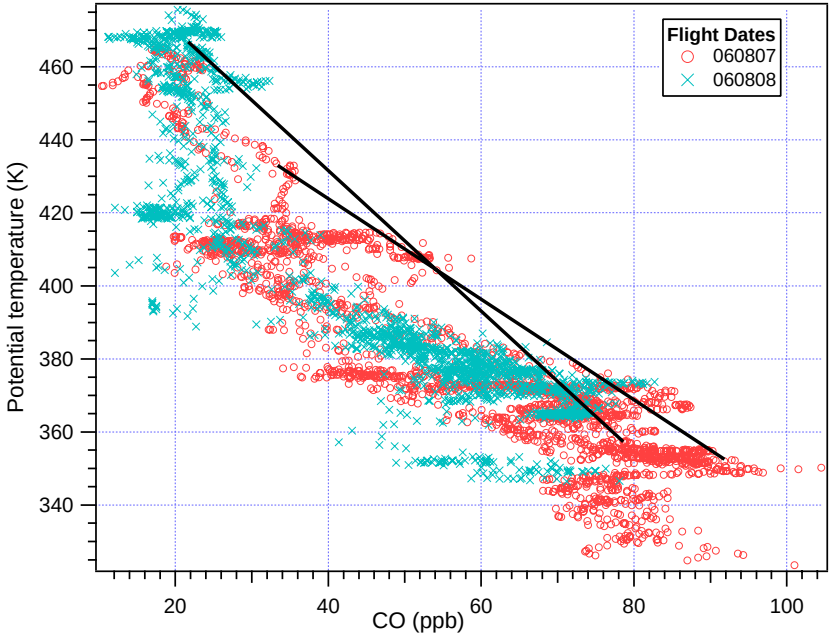

Fig. 6. CO profiles for 7 and 8 August. The black lines represent the two most extreme possible mixing lines that could explain the high CO values at 410 K. One mixing line would mean mixing of air parcels with a potential temperature of 355 K and 430 K, the other line mixing of air parcels with potential temperatures of 355 K and 470 K. Any mixing line in between these two extremes is possible to explain the enhanced CO values at 410 K.

ACPD
9, 25049–25084, 2009

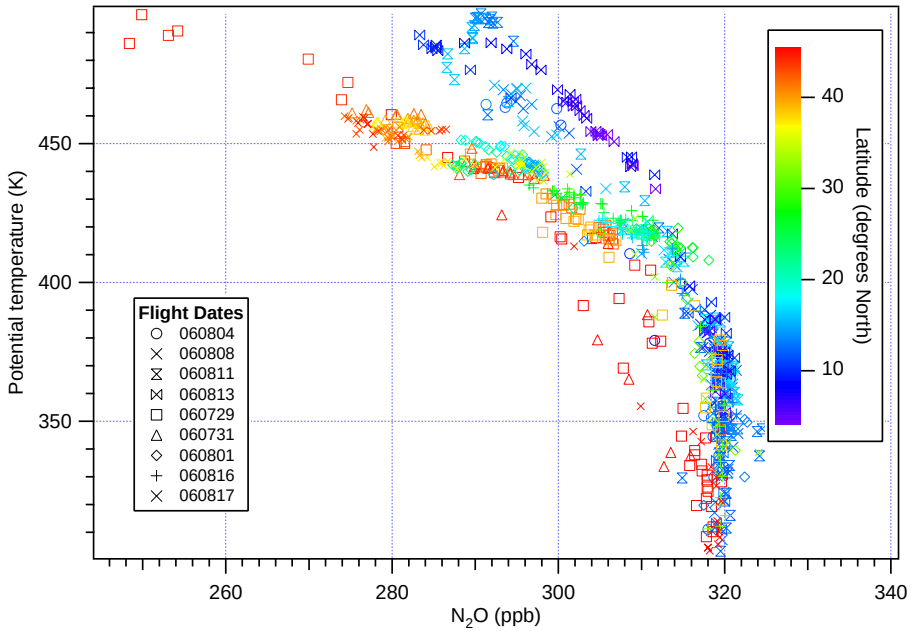

Fig. 7. Vertical profile of N_2O coloured to latitude.

ACPD
9, 25049–25084, 2009

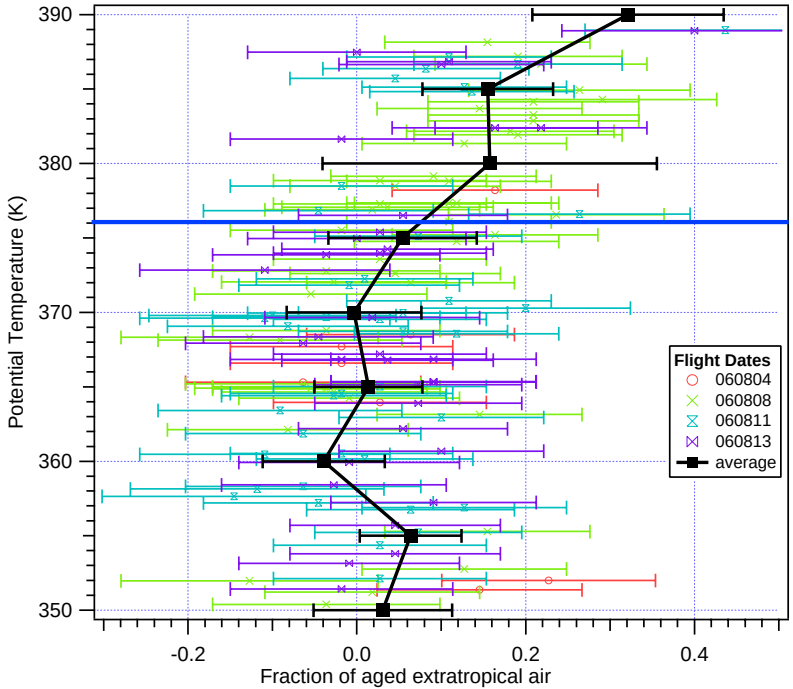

Fig. 8. Fraction of aged extratropical air for each measurement. Black line: average fraction for all four flights. Blue line: average height of the tropopause.

ACPD
9, 25049–25084, 2009

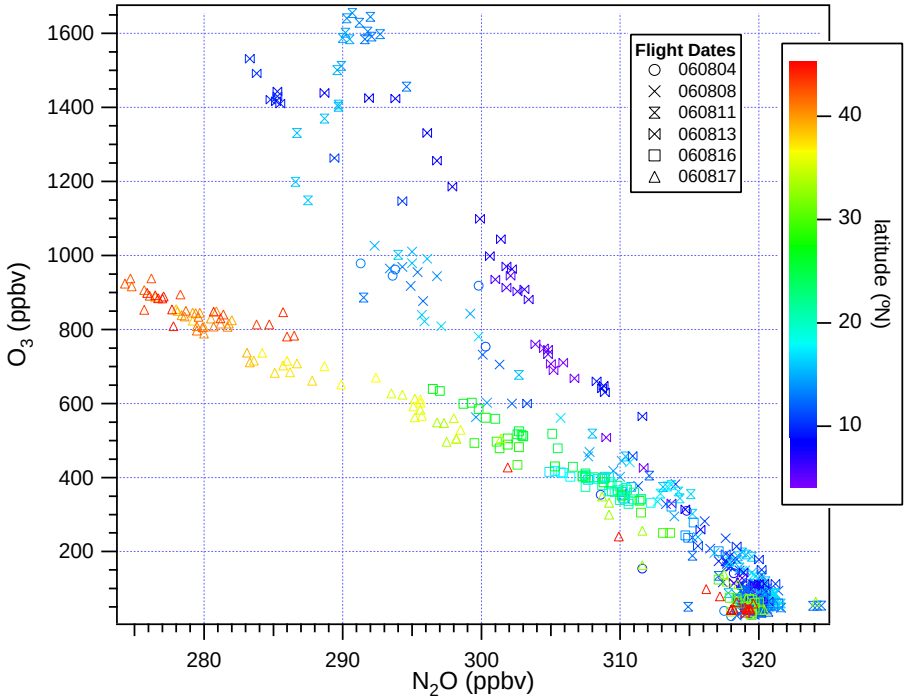

Fig. 9. Correlation between N_2O and O_3 coloured to latitude.

ACPD
9, 25049–25084, 2009

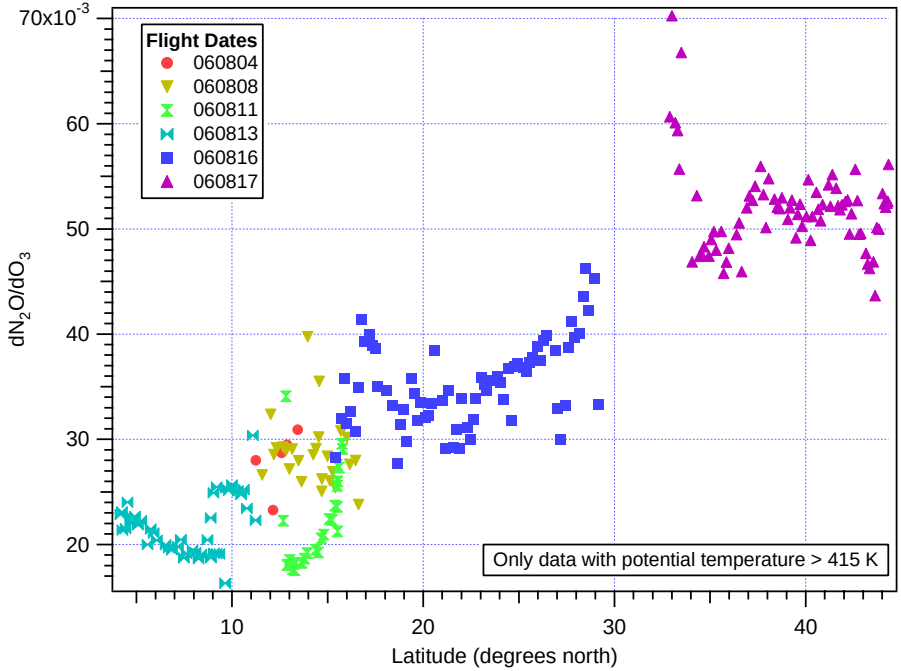

Fig. 10. Slope dN_2O/dO_3 as a function of latitude for the local AMMA/SCOUT-O3 flights and the two transfer flights from Ouagadougou to Verona (Italy).

ACPD
9, 25049–25084, 2009

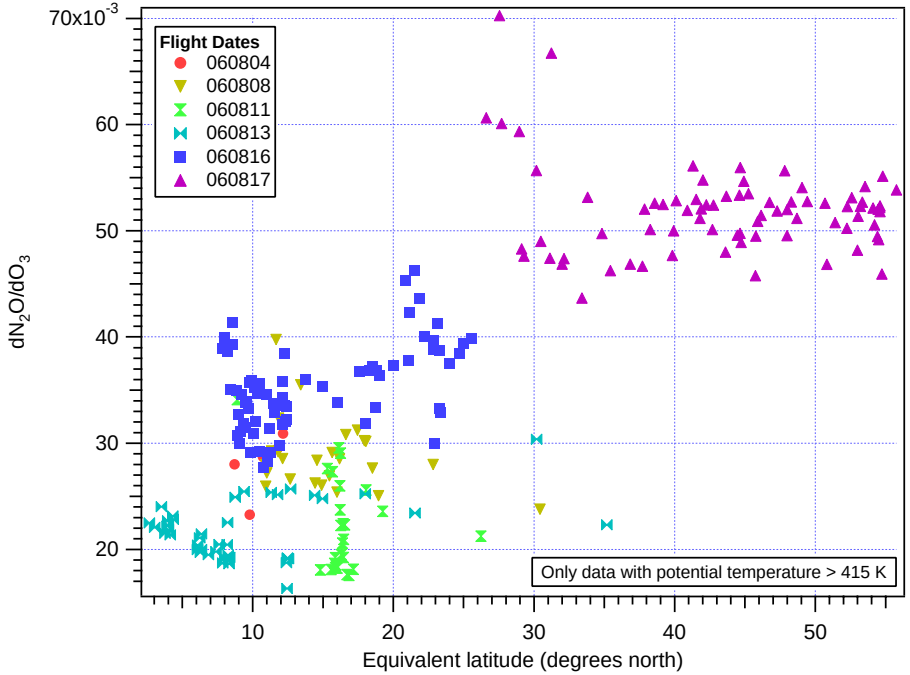

Fig. 11. Slope dN_2O/dO_3 as a function of equivalent latitude for the local AMMA/SCOUT-O3 flights and the two transfer flights from Ouagadougou to Verona (Italy).

ACPD
9, 25049–25084, 2009

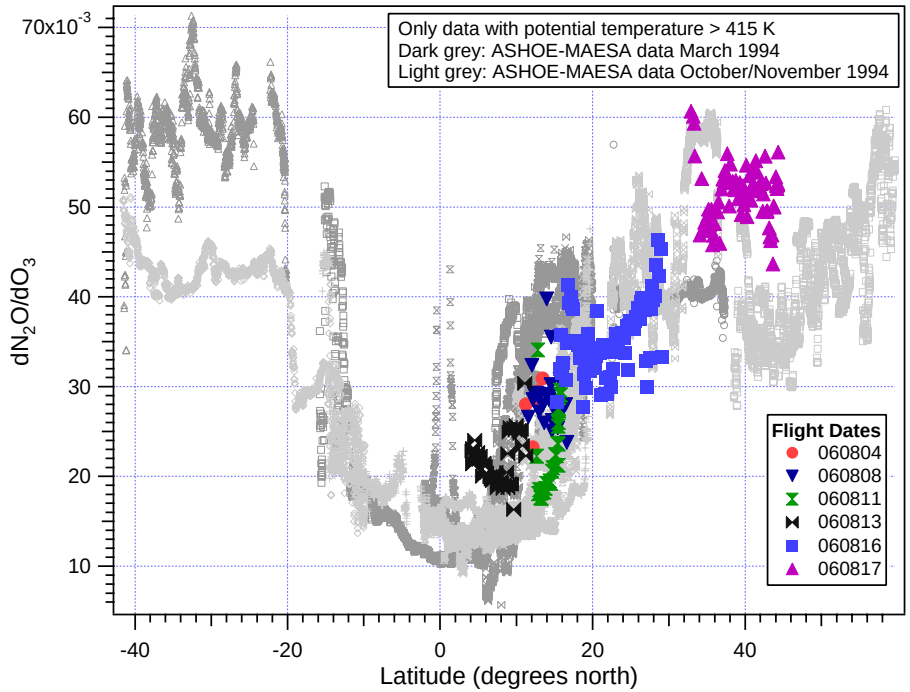

Fig. 12. Slope of dN_2O/dO_3 as a function of latitude for the AMMA/SCOUT-O3 flights (coloured) and ASHOE/MAESA (grey).

ACPD
9, 25049–25084, 2009